On the determination of the primary part of the seismically induced inertial forces in pressurized piping systems

Axel Méric, Pierre Labbé, Djaffar Boussaa, Jean-François Semblat, Pierre-Alain Nazé

▶ **To cite this version:**

Axel Méric, Pierre Labbé, Djaffar Boussaa, Jean-François Semblat, Pierre-Alain Nazé. On the determination of the primary part of the seismically induced inertial forces in pressurized piping systems. SMiRT 27 - 27th International Conference on Structural Mechanics in Reactor Technology, Mar 2024, Yokohama, Japan. hal-04690802

HAL Id: hal-04690802
https://hal.science/hal-04690802

Submitted on 6 Sep 2024

HAL is a multi-disciplinary open access archive for the deposit and dissemination of scientific research documents, whether they are published or not. The documents may come from teaching and research institutions in France or abroad, or from public or private research centers.

L'archive ouverte pluridisciplinaire **HAL**, est destinée au dépôt et à la diffusion de documents scientifiques de niveau recherche, publiés ou non, émanant des établissements d'enseignement et de recherche français ou étrangers, des laboratoires publics ou privés.

Transactions of the SMiRT 27
Yokohama, Japan, March 3-8, 2024
Division IV

On the determination of the primary part of the seismically induced inertial forces in pressurized piping systems

Axel Méric[1], Pierre Labbé[2], Djaffar Boussaa[3], Jean-François Semblat[4], Pierre-Alain Nazé[1]

[1]Geodynamique & Structure, Montrouge, France (axel.meric@geodynamique.com)
[2]IRC, ESTP Paris, Cachan, France
[3]LMA AMU CNRS Centrale (UMR7031), Marseille, France
[4]IMSIA (UMR9219), CNRS, EDF, CEA, ENSTA Paris, Institut Polytechnique de Paris, France

ABSTRACT

This paper focusses on discussing which part of inertial stresses should be regarded as primary or secondary. To do so, a classification is established based on the study of non-linear oscillator. The case of zero and non-zero-permanent force are explored to simulate the pressure effect. Two types of dynamic signals are considered as samples of a wide-band and a narrow-band stochastic process to simulate ground level motions and floor input motions respectively. The results of the classification highlight the importance the parameter φ parameter, the ratio between the natural frequency of the oscillator and the central frequency of the input motion, in the calculation of the primary part of the inertial forces. Based on the defined classification, a reduced spectrum method, initially proposed by Labbé and Nugyen *[Modified Response Spectrum Accounting for Seismic Load Categorization as Primary or Secondary in Multi-Modal Piping Systems, ASME 2021, PVP]* is tested numerically on a piping system. Non-linear calculations are compared to the results of the linear reduced spectrum analysis. Von-mises stresses at the most damaged elbow flank and opening/closing displacement of the same elbow are compared. Comparable results are obtained in term of stresses.

INTRODUCTION

In the current post Fukushima international context, seismic levels are often reassessed, sometimes by a factor two or more. In these conditions, the design justification of pressurized piping systems can be tricky. The purpose of this paper is to address the issue of piping system design margins, in the wake of research perspectives on the subject, identified by the OECD (2018).

In standards (ASME, RCCM), seismically induced inertial stresses are almost always regarded as primary stresses and are evaluated through linear spectral analysis. Based on the analysis of seismic responses of a series of elastic-plastic oscillators, this paper focusses on discussing which part of inertial stresses should be regarded as primary. Two types of input motions are considered: samples of a wide-band stochastic process to simulate ground level seismic motions, and samples of narrow-band stochastic process to simulate floor input motions. In addition, oscillators with an applied non-zero static force are considered, to simulate the pressure effect.

Previous research was carried out by Labbé (2020), addressing the case of wide-band input with no pressure. A major output was the crucial role played by the φ parameter (ratio between the natural frequency of the oscillator and the central frequency of the input motion) in margin assessment. A development of the method was presented by Labbé and Nguyen (2021), who introduced the concept of reduced spectrum.

CONSIDERED INPUT MOTIONS

Ground motion samples are defined by their power spectral density (PSD), which consists in a filtered one-sided truncated white noise, S_0, defined on the [0 Hz, 50 Hz] frequency interval. As proposed by Nguyen (2017), this white noise is filtered by a Kanai-Taijimi (Tajimi, 1960) filter, a Clough and

Penzien (1975) filter to reduce the low frequency content of the motion, and a low-pass filter to control the high frequency content. The resulting PSD is displayed in Equation (1), with subscripts KT, CP, and LP refereeing respectively to the Kanai-Tajimi, the Clough and Penzien and the low-pass filter transfer functions parameters:

$$S(\omega) = \frac{1 + 4\xi_{KT}^2\Omega_{KT}^2}{(1-\Omega_{KT}^2)^2 + 4\xi_{KT}^2\Omega_{KT}^2} \frac{\Omega_{CP}^2}{(1-\Omega_{CP}^2) + 2i\xi_{CP}\Omega_{CP}} \frac{1/\omega_{LP}^2}{(\Omega_{LP}^2 - 1) + 2i\xi_{LP}\Omega_{LP}} \; S_0$$
$$\text{with } \Omega_{KT} = \frac{\omega}{\omega_{KT}} \; ; \; \Omega_{CP} = \frac{\omega}{\omega_{CP}} \; ; \; \Omega_{LP} = \frac{\omega}{\omega_{LP}} \; ; \; \omega = 2\pi f \tag{1}$$

The signal generation procedure is described in Labbé (2021). Each sample $\gamma_i(t)$ last 20 seconds and the strong phase of each signal is controlled by a time-envelope curve $E(t)$ of α-type (Jennings, et al., 1968) whose expression is:

$$E(t) = \alpha_1 t^{(\alpha_2 - 1)} \exp(-\alpha_3 t) \tag{2}$$

Regarding the narrow-band input samples, they are obtained as top floor responses of a five-storey building, subjected at the base to the above ground motion samples. In the model, the five storeys have the same stiffness and the five floors the same mass. It is assumed that the response is only controlled by the first mode (which carries 88% of the total mass), whose eigen frequency is $f_1 = 3.2\ Hz$, and damping to critical value $\xi_1 = 0.05$.

One thousand samples of wide-band samples are generated, and one thousand narrow-band samples derived. Their non-dimensional mean PSD and mean response spectra are presented in Figure 1 and Figure 2. The response spectrum peak frequency is 2.7 Hz for the wide-band and 3.2 Hz for the narrow-band process. We present the non-dimensional spectra because, in a next step, every sample is calibrated at different levels, as presented further.

Table 1: Input motions parameters

-	Parameter	Value	Unit
Frequency range	-	0.05 - 50	[Hz]
Kanai-Tajimi filter	f_{KT}	2.5	[Hz]
	ξ_{KT}	0.5	[-]
Clough and Penzien filter	f_{CP}	0.125	[Hz]
	ξ_{CP}	1	[-]
Low-pass filter	f_{LP}	10	[Hz]
	ξ_{LP}	1	[-]
Time envelope curve	α_1	1.33	[-]
	α_2	2.5	[-]
	α_3	0.5	[-]
Structure to obtain narrow band signals	Number of story	5	[-]
	ξ_1	0.05	[-]
	f_1	3.2	[Hz]

Processing PSDs enables to calculate the central frequency, f_c, and bandwidth, δ_1, of each series of samples, according to classical random vibration theory formulas reported in Equations (3) and (4), where m_i the spectral moment of order i of $S(\omega)$.

According to classical random vibration theory formulas reported in Equations (3) and (4), where m_i the spectral moment of order i of $S(\omega)$, processing PSDs enables to calculate the central frequency, f_c, and bandwidth, δ_1, of each series of samples, (Values presented in Table 2.)

$$f_c = \frac{1}{2\pi}\sqrt{\frac{m_2}{m_0}} \tag{3}$$

$$\delta_1 = \sqrt{1 - \frac{m_1^2}{m_0 m_2}} \tag{4}$$

Table 2: Input motions statistics

Parameter	Unit	Wide band signal	Narrow band signal
Cenral frequency	[Hz]	3.17	3.35
Peak frequency	[Hz]	2.20	3.2
Bandwidth δ_1	[-]	0.59	0.19

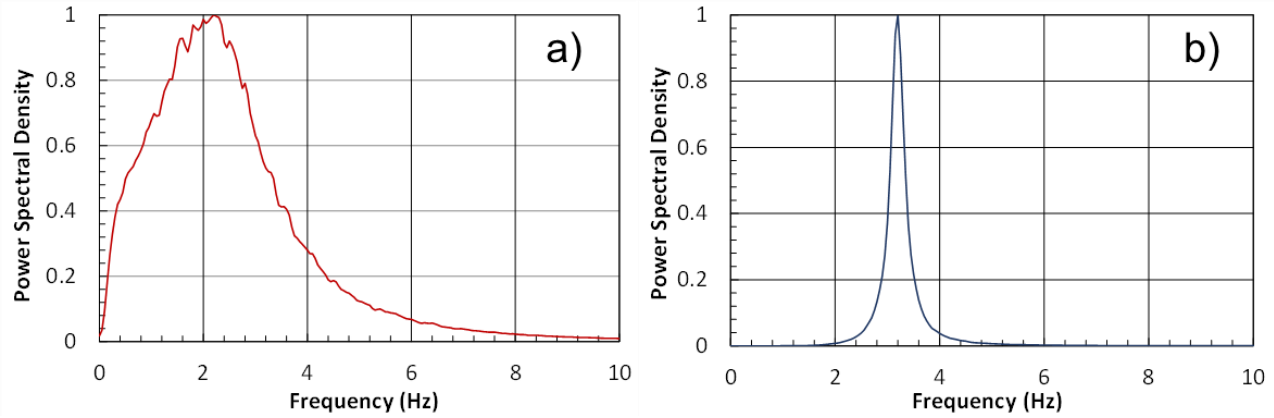

Figure 1: Mean PSD of: a) Wide band signals, b) Narrow band signals

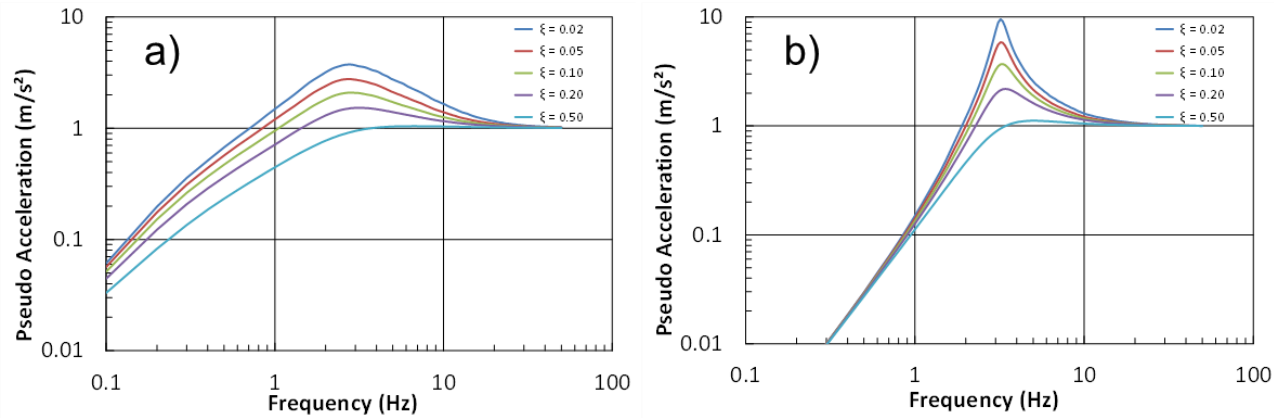

Figure 2: Mean pseudo acceleration response spectrum of: a) Wide band signals, b) Narrow band signals

THE ELASTIC-PLASTIC OSCILLATOR

Considering an elastic-plastic oscillator, its response is the sum of an elastic part, X_e, and a plastic part X_p such that $X_{tot} = X_e + X_p$. The equation of motion reads as per Equation (5), where ξ_0 is the viscous damping ratio to critical, ω_0 the circular frequency, F the spring "force", and γ the input motion, which can be a sample of a wide band, or a narrow band signal as defined previously. Then, F is given by Equation (6).

$$\ddot{X}_{tot} + 2\xi_0\omega_0\dot{X}_{tot} + F(X_{tot}) = -\gamma(t) \tag{5}$$

$$F(X_{tot}) = \omega_0^2\left(X_{tot} - X_p\right) \tag{6}$$

A single constitutive relationship is considered in this paper, the Linear Kinematic Hardening (LKH) or Prager model (1955). This time-independent dissipative relationship is reasonably representative of steel structures behavior., the studied plastic law is described below, with the definition of the Von-Mises yield criteria F_y and the flow rule $\dot{X}_p$ in the case of one-dimensional plasticity.

$$F_y = |F - q| - F_0 \tag{7}$$

$$\dot{X}_p = \Lambda\, sign(F - q) \tag{8}$$

$$\dot{q} = \alpha k_0 \dot{X}_p \tag{9}$$

The complementarity conditions, $\Lambda \geq 0, F_y \leq 0, \Lambda F_y = 0$, apply for this model.

In the above, F_0 is the yield force, Λ the plastic multiplier, q the elasticity domain translation, k_0 is the initial oscillator stiffness.

A series of oscillators are retained, on which a parametric study of their elastic-plastic responses is conducted. Their features are as follows:

- The major feature is the elastic frequency, f_0. For every input motion a set of six f_0 values are selected, such that the non-dimensional frequency, $\varphi = f_0/f_c$ (f_c is the central frequency of the considered input motion.), takes values $\varphi = \{0.1, 0.2, 0.5, 1.0, 2.0, 5.0\}$, ranging the studied oscillators relative stiffness from flexible to stiff.
- Two α values are considered, $\alpha = 0.1$ and $\alpha = 0.2$.
- A common 5% ξ_0 value is chosen for all oscillators.
-

STRESS CATEGORIZATION

The principle of stress categorization is presented in Labbé (2018) and Labbé and Nugyen (2021). We consider a simple oscillator of yield strength F_0 and yield displacement D_0, ultimate strength F_u and ultimate displacement D_u. We introduce the non-dimensional parameters η_u and μ_u representing the hardening and ductility capacity:

$$\eta_u = \frac{F_u}{F_0} \tag{10}$$

$$\mu_u = \frac{D_u}{D_0} \tag{11}$$

Let's consider now a seismic input motion $\Gamma(t)$. We define $\Gamma_0(t)$ as the calibrated $\Gamma(t)$ seismic input motion that brings the oscillator at the yield limit ($\max(|F(t)|) = F_0$; $\max(|D(t)|) = D_0$). Then we designate $\Gamma_u(t)$ the same input motion, such calibrated that it brings the oscillator to its ultimate capacity. We introduce $\lambda_u = \Gamma_u(t)\,/\Gamma_0(t)$. It is clear that:

- If $\lambda_u = \eta_u$, the seismic motion can be considered as force-controlled load, and concurrently, seismically induced inertial stresses should be regarded as purely primary;
- If $\lambda_u = \mu_u$, the seismic motion can be considered as displacement-controlled load, and concurrently, seismically induced inertial stresses should be regarded as purely secondary.

Realistically, a seismic input motion should not be regarded as purely primary or purely secondary. In Labbé (2018), the parameter τ_P was introduced such that the primary part σ_P of the seismically induced stress σ, obtained as an output of conventional elastic analysis, is expressed as per Equation (13), where τ_P is given by Equation (14). At this stage, it is convenient to introduce the parameter m, defined by Equation (15), which can be interpreted as a secondarity index.

$$\sigma_P = \tau_P \sigma \tag{12}$$

$$\tau_P = \frac{\eta_u}{\lambda_u} \tag{13}$$

$$\tau_P = \left(\frac{\eta_u}{\mu_u}\right)^m \tag{14}$$

To determine the value of m, a numerical statistic study is carried out on the above introduced series of elastic-plastic oscillators. One thousand samples of a wide input motion and one thousand samples of a narrow input motion are considered. For every oscillator, eleven λ_u values are considered, corresponding to increasing levels of input motion. In addition, three F_P values are considered, corresponding to zero, one-third, and to two-thirds of the yield strength. The numerical study is summed up in figure 3. In total, 792 000 results are obtained, for which the secondarity index is calculated according to Equation (15).

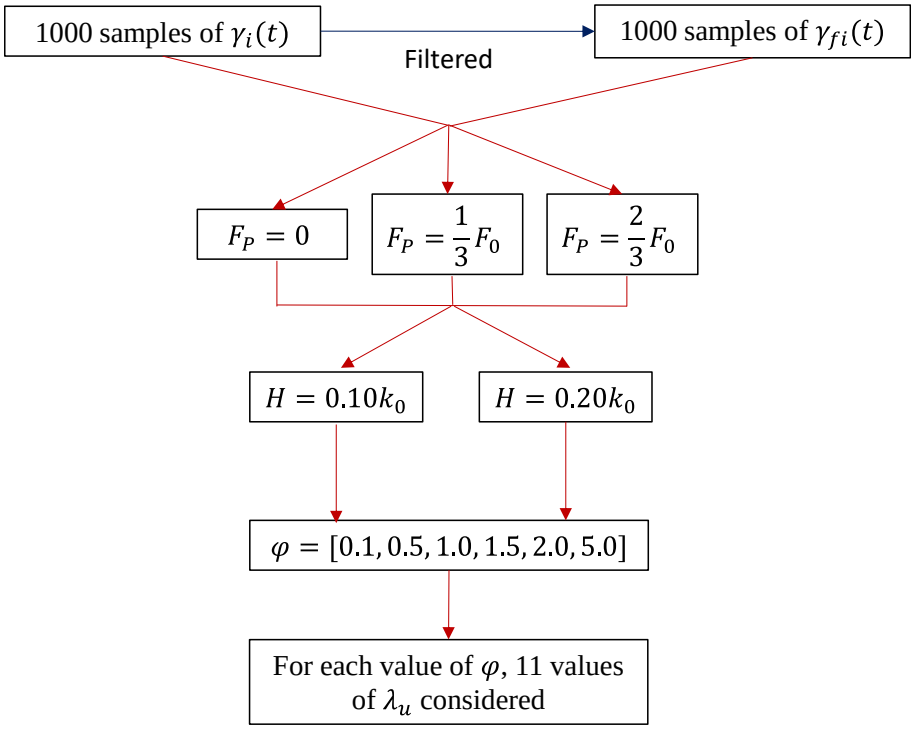

Figure 3: Numerical experimental scheme

The mean value of the secondarity index is calculated for each value of φ. To practical use, as it has been done in Labbé and Nguyen (2021), the parameter $\psi = f_0/f_p$ is introduced, which is the ratio of the oscillator natural frequency f_0 over the response spectra peak frequency f_p. Since the seismic input motion is often viewed in terms of response spectrum, the seismic motion central frequency f_c could be harder to identify in engineering practice compared to the response spectrum peak frequency f_p. The mean values of m are plotted versus ψ for each type of input motion, each value of α and each value of F_P, in figure 4 and 5.

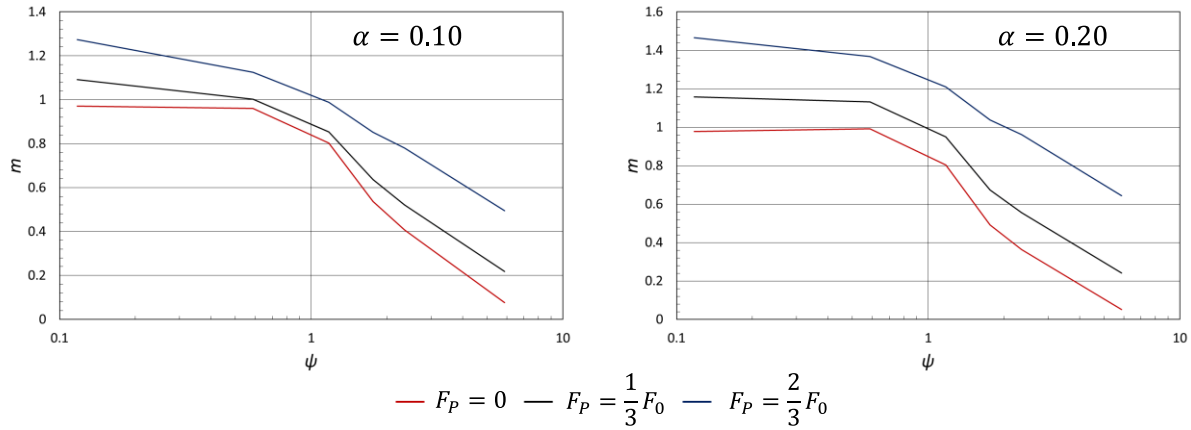

Figure 4: mean values of the secondarity index m in the case of wide band input motions

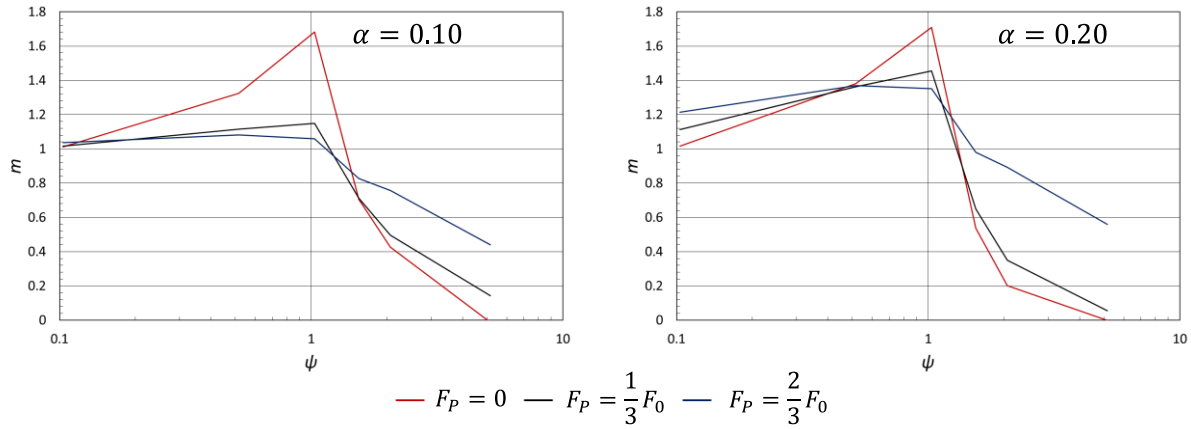

Figure 5: mean values of the secondarity index m in the case of narrow band input motions

The results show the dependence of the secondarity index m on the non-dimensional frequency ψ as already highlighted by Nguyen (2017) and Labbé and Nguyen (2021). In addition, as already reported by Labbé (1994), a peak can be observed for $\psi = 1$ in case of narrow band, whereas there is no peak in case of wide band input motions. Regarding F_P, it tends to translate the curves upward in case of wide band input, and, on the opposite, to reduce the peak in case of narrow band input motion. The α value has some influence, although not crucial.

Regarding the results in the case of wide band input motions with a zero permanent force, an engineering method based on modal spectral analysis was proposed by Labbé and Nguyen (2021) to assess the inertial primary stresses of monomodal and multimodal piping systems. They proposed a general evolution for $m(\psi)$ represented in figure 6. The evolution of $m(\psi)$ leads to the evolution of $\tau_P(\psi)$ for a fixed η_u/μ_u value according to equation 15. The primary part $\sigma_{P,i}$ of the inertial stress

σ_i obtained by the contribution of the mode i of frequency f_i is calculated according to equation 15 by calculating $\tau_{P,i}$ as follows:

$$\tau_{P,i} = \tau_P(\psi_i) = \tau_P\left(\frac{f_i}{f_p}\right) \tag{15}$$

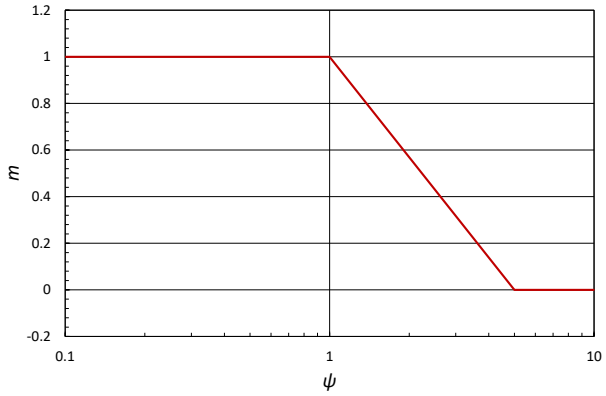

Figure 6: General evolution of $m(\psi)$

Alternatively, $\tau_{P,i}$ can be regarded as a coefficient applied on the input response spectrum. The following rule was proposed by Labbé and Nguyen (2021):

$$\begin{aligned}
&- if\ f \le f_p && \begin{cases} if\ (\eta_u/\mu_u)^m \ge S_{ZPA}/S_p : S'(f) = \tau_P\left(\frac{f}{f_p}\right) S(f) \\ else \qquad\qquad S'(f) = S_{ZPA} \end{cases} \\
&- if\ f_p < f < f_{ZPA} && linear\ \log - \log\ scale\ between\ S'(f_p)\ and\ S'(f_{ZPA}) \\
&- if\ f \ge f_{ZPA} && S'(f) = S_{ZPA}
\end{aligned}$$

In the above, $S(f)$ is the input response spectrum, $S'(f)$ the reduced response spectrum, S_p and S_{ZPA} respectively the peak value and zero period acceleration of $S(f)$. The frequency f_{ZPA} is the minimum value of f such that $S(f) = S_{ZPA}$. A prudent approach was made to avoid that $S'(f_p)$ be lower that S_{ZPA}.

Let's admit for the rest of the study that the macroscopic behavior of a pressurized piping system can be idealized as a $\alpha = 0.20$ LKH oscillator submitted to a permanent load equal to $F_P = \frac{2}{3}F_0$. In this situation, we define $m_{20}(\psi)$ as the specific secondarity index of this oscillator/elbow. The evolution of $m_{20}(\psi)$ is the result of the numerical study previously made on oscillator, it has been plotted in figure 4 and 5. Then, we define as NRRS the non-reduced response spectrum classic method to determine σ. We define as LNRRS the Labbé and Nugyen (2021) reduced response spectrum method defined above, that uses the general $m(\psi)$ evolution defined in figure 6. We denote as KHRRS the kinematic hardening reduced response spectrum method which considers the experimental evolution $m_{20}(\psi)$ defined previously to calculate the reduced spectrum, such that $\tau_{P,i} = \tau_{P,i}(m_{20}(\psi_i))$. This method follows the same algorithm than the one proposed by Labbé and Nguyen (2021) for the LNRRS method. But, one difference is made between the LNRRS and the KHRRS algorithm: no limit is considered on the value of $S'(f_p)$ for the KHRRS method ($S'(f_p) < S_{ZPA}$ is allowed). This limit was imposed by Labbé and Nguyen (2021) for safety purposes, they also discussed the eventuality of removing this condition. This is tested in this paper. Some results of these three methods are presented in the next section.

THE BARC PIPING SYSTEM

The steel pressurized piping system example studied in this section is taken from Ravikiran et al. (2015). It is chosen because its geometry and material properties are representatives of an industrial piping system. This is a monomodal piping system. The pipes outer diameter is 168mm and the thickness is 7mm, the elbow radius of curvature is 228m. The pressure is equal to 6 MPa. The finite element model, composed of around 10000 shell elements, is represented in figure 7. The materials behavior is defined in Ravikiran et al. (2015), Chaboche (1991) non-linear kinematic hardening is used to describe the plastic behavior. To evaluate the above LNRRS and KHRRS methods, non-linear transient analyses and linear spectral analyses are performed on this system. The considered input motions are samples of wide band and narrow band motions defined in the first section.

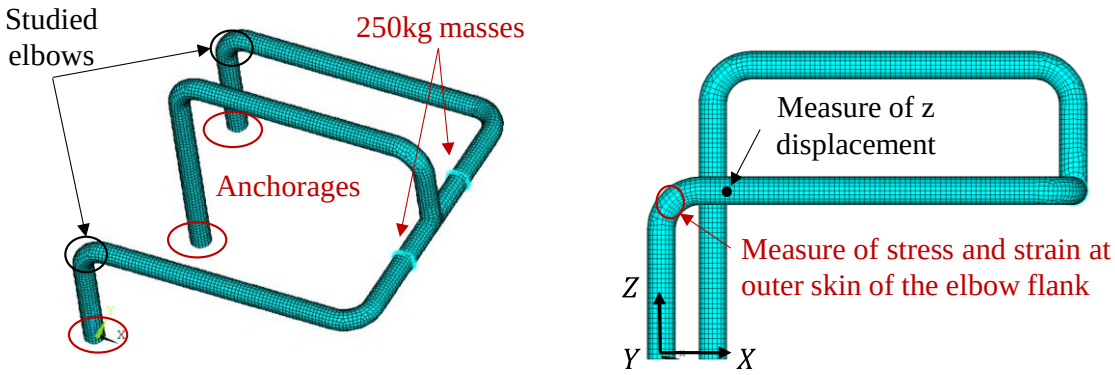

Figure 7: Finite element model of the BARC (Ravikiran et al., 2015) piping system

The volumic mass of steel is adjusted to induce the first mode frequency equal to $f_1 = 3.20\,Hz$ such that $f_0/f_c \approx 1.0$ for the wide band and narrow band input motions defined in the first section. It induces values of $\psi_W = 3.2/2.7 = 1.19$ and $\psi_N = 1.0$ in the case of wide band and narrow band input motions respectively. The first mode of the structure is the one that open/close the studied elbows circled in figure 7. One sample of the wide band input motion and one sample of the narrow band input motions are considered for the loadings. They are applied in the Z direction. Four values of λ_u are considered for each type of signal. These values are $\lambda_u = [1, 5, 10, 20]$. The value $\lambda_u = 1$, like $\Gamma_0(t)$ defined previously, represents the case of the input motion that bring the studied elbow at the yield limit. The response spectra for $\lambda_u = 10$ are shown for both types of input motions in figure 8. The results of the non-linear transient calculations are listed in table 3. The results are the von-mises stress and the circumferential strain located at the outer skin of the studied elbow flank. The Z displacement of opening/closure is also reported.

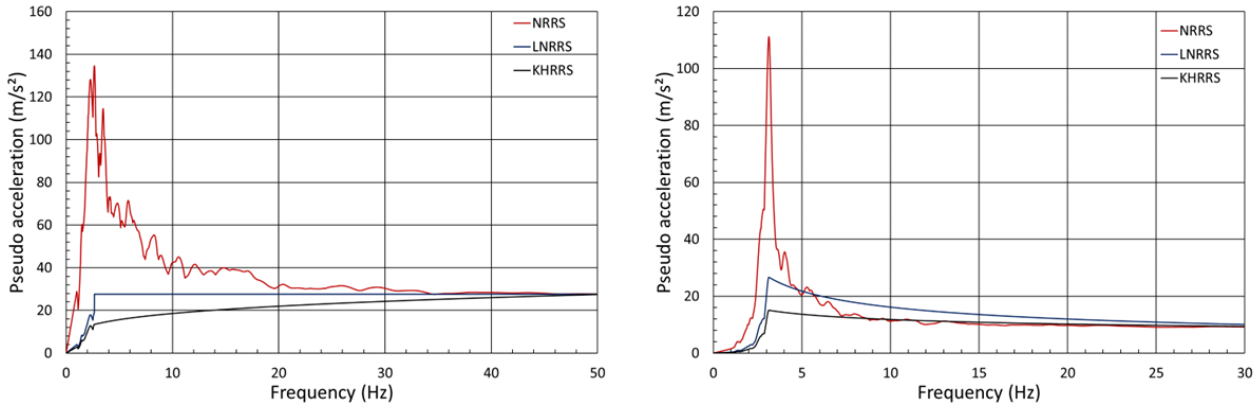

Figure 8: 3% response spectrum for $\lambda_u = 20$ – Left: wide band signal – Right: narrow band signal

Table 3: Results of non-linear calculations

Type of signal	Wide Band				Narrow Band			
Amplification	λ=1	λ=5	λ=10	λ=20	λ=1	λ=5	λ=10	λ=20
Von-Mises Stress at elbow flank (MPa)	235	306	345	436	235	300	325	346
Circumferential stain at elbow flank (%)	0.1	0.45	0.94	2.7	0.1	0.43	0.74	1.27
Elbow opening/closure (mm)	2.4	7.8	12.5	32	2.4	7.7	11	15

Based on the non-linear calculations, the reduced spectrum approach is tested. The reduced spectra are presented in figure 8. The results are presented int table 4 and 5. The mentioned ratio is the ratio of the linear/equivalent linear response over the nonlinear response. As expected, the classical NRRS approach overpredict the primary stresses. The LNRRS results are overall in good accordance with the non-linear ones. The results for $\lambda_u = 20$ are less accurate because of the condition imposing $S'(f_p) = S_{ZPA}$. On the contrary, the KHRRS approach, that has not this condition imposed, give very good results compared to the non-linear ones. The narrow-band input motion with $\lambda_u = 20$ was not as well predicted as the others cases. Displacements are underpredicted by the method, as expected by the choice of an equivalent linear study that aims to predict the correct state of stress and which is based on a scalar reduction of the loadings.

Table 4: Reduced spectrum approach results for wide band input motions

Type of signal	Wide Band Input Motions								
Amplification	λ=5			λ=10			λ=20		
η_u/μ_u	0.41			0.28			0.14		
Method	NRRS	LNRRS	KHRRS	NRRS	LNRRS	KHRRS	NRRS	LNRRS	KHRRS
Von-Mises Stress at elbow flank ratio	2.00	1.14	1.06	3.54	1.45	1.04	5.59	1.80	1.06
Elbow opening/closure ratio	0.90	0.53	0.45	0.98	0.43	0.31	0.75	0.25	0.15

Table 5: Reduced spectrum approach for narrow band input motions

Type of signal	Narrow Band Input Motions								
Amplification	λ=5			λ=10			λ=20		
η_u/μ_u	0.40			0.30			0.24		
Method	NRRS	LNRRS	KHRRS	NRRS	LNRRS	KHRRS	NRRS	LNRRS	KHRRS
Von-Mises Stress at elbow flank ratio	2.14	1.09	0.90	3.94	1.42	1.02	7.35	2.06	1.26
Elbow opening/closure ratio	0.91	0.47	0.36	1.19	0.45	0.31	1.68	0.50	0.31

CONCLUSION

A categorization of stresses has been presented based on the study of elasto-plastic oscillators. A method to determine the primary part of inertial stresses is proposed, it is dependent on the ratio φ of the natural frequency of the oscillator over the central frequency of the input motion. It is also dependant on the input motion bandwidth and the value of the permanent force.

The proposed reduced spectrum approach based on the presented stress categorization has been tested on the Ravikiran et al. (2015) piping system. Results of stresses were in good accordance with the ones obtained by a non-linear transient analysis. The studied piping system is monomodal. The authors recognize the importance to test this method on multimodal piping systems in future work as the approach was originally thought by Labbé and Nguyen (2021) to be used for these situations.

REFERENCES

Chaboche, J.L. (1991). On some modifications of kinematic hardening to improve the description of ratchetting effects. Int. J. Plast. 7.

Clough, R. W., and Penzien, J. (1975). Stochastic response of linear MDOF systems, Dynamics of structures, McGraw–Hill, New York.

OCDE (2018). Integrity of Structures, Systems and Components Under Design and Beyond Design Loads in Nuclear Power Plants. NEA/CSNI/R (2018)3. https://www.oecd-nea.org/nsd/docs/2018/csni-r2018-3.pdf.

Labbé, P. (1994). Ductility demand and design of piping systems, 10th European Conference on Earthquake Engineering, August 1994, Vienna.

Labbé, P. (2018). On Categorization of Seismic Load As Primary or Secondary for Piping Systems with hardening capacity, proceedings of the ASME 2018 Pressure Vessels and Piping Conference, American Society of Mechanical Engineers, July 15-20, 2018, Prague.

Labbé, P. (2020). On Categorization of Seismic Load As Primary or Secondary for Multi-Modal Piping Systems, in: Volume 9: Seismic Engineering. Presented at the ASME 2020 Pressure Vessels & Piping Conference, American Society of Mechanical Engineers, Virtual, Online, p. V009T09A001.

Labbé, P., Nguyen, T.A. (2021). Modified Response Spectrum Accounting for Seismic Load Categorization as Primary or Secondary in Multi-Modal Piping Systems, in: Volume 5: Operations, Applications, and Components; Seismic Engineering; Non-Destructive Examination. Presented at the ASME 2021 Pres-sure Vessels & Piping Conference, American Society of Mechanical Engineers, Virtual, Online, p. V005T08A006.

Nguyen, T.A. (2017). Analyse systématique du concept de comportement linéaire équivalent en ingénierie sismique, PhD., université Paris-Est, ESTP, Cachan.

Ravikiran, A., Dubey, P. N., Agrawal, M. K., Reddy, G. R. (2018). Experimental and numerical studies of ratcheting in pressurized stainless steel piping systems under seismic load, BARC/2015/E/018.

Tajimi, H. (1960). A statistical method of determining the maximum response of a building structure during an earthquake. In Proceedings of the 2nd World Conference on Earthquake Engineering, Tokyo, Japan, pages 781–797.